

# Renewable diesel blendstocks produced by hydrothermal liquefaction of wet biowaste

Wan-Ting Chen<sup>1</sup>, Yuanhui Zhang<sup>1,2\*</sup>, Timothy H. Lee<sup>3</sup>, Zhenwei Wu<sup>1</sup>, Buchun Si<sup>1,2</sup>, Chia-Fon F. Lee<sup>3</sup>, Alice Lin<sup>1</sup> and Brajendra K. Sharma<sup>4</sup>

**Processing wet biowaste to create a useful product, a practice called valorization, is environmentally sustainable and has the potential to augment energy production. Biocrude converted from wet biowaste using hydrothermal liquefaction (HTL) has comparable heating values to petroleum crude. However, its composition is too complex for use as transportation fuels. Here, we show that distillation combined with esterification can effectively upgrade HTL biocrude oil into diesel blendstock. We demonstrate that the HTL biocrude oil converted from food processing waste and animal manure can be distilled into fractions with similar energy content to that of petroleum diesel. We then reduce the acidity of distillates through esterification to meet the diesel standard. Engine tests performed using 10–20% upgraded distillates blended with diesel show 96–100% power output, 101–102% NO<sub>x</sub>, 89–91% CO, 92–125% unburned hydrocarbon and 109–115% soot emissions, compared with regular diesel. HTL integrated with distillation and esterification has a higher energy recovery ratio than anaerobic digestion, lipid extraction, HTL combined with hydrotreating and producing diesel from petroleum. This approach realizes the potential of wet biowaste to alleviate petroleum consumption and to reduce greenhouse gas emissions.**

Wet biowaste-to-energy conversion, especially to high-value transportation fuels, is of rising interest. The United States annually produces 79 million dry tons of wet biowaste from food processing and animal production<sup>1,2</sup>. The energy content of wet biowaste streams ( $\sim 1.3 \times 10^{12}$  MJ) is about 60% of the current US renewable biofuel energy production ( $\sim 2.2 \times 10^{12}$  MJ)<sup>2</sup> (<https://www.eia.gov>), but is not effectively harvested. The high water content (80–99%) of wet biowaste is a major bottleneck, preventing many bioenergy conversion technologies from achieving a net positive energy balance. Life cycle analyses have shown that drying biowaste for conventional solvent extraction techniques consumes about 90% of the energy content of the recoverable oils<sup>3,4</sup>. With wet biowaste rapidly increasing due to urbanization, industrialization and growing population, finding an effective means of repurposing biowaste becomes increasingly crucial<sup>2,5</sup>. Moreover, the World Bank has projected a 70% global increase in urban waste and an 83% increase treatment cost by 2025<sup>6</sup>. Treating biowaste will become increasingly expensive, particularly for developing countries. It will cost developing countries about 2% of global gross domestic product to treat the human waste<sup>7,8</sup>. Consequently, a paradigm shift to consider biowaste as a resource rather than a waste is key for a sustainable future.

HTL is well suited for the valorization of wet biowaste because it (1) uses water as the reaction medium and (2) converts non-lipid components into biocrude oil<sup>5,9</sup>. Unlike the production of conventional biodiesel from lipid-containing feedstocks such as soybean, HTL enables efficient energy recovery from the downstream of the human food chain, avoiding competition between bioenergy production and farmland and food supply<sup>9,10</sup>. HTL has been proven to convert 30–70% of organic components into biocrude oil with heating values of 32–38 MJ kg<sup>-1</sup> (75–90% of the petroleum heating

value)<sup>11,12</sup> at various temperatures (260–320 °C)<sup>13–15</sup>, reaction times (15–120 min)<sup>13–15</sup> and water contents (65–90%)<sup>16</sup>.

Biocrude oil converted from biowaste contains 26–44 wt% distillation fractions that, with further upgrading, are suitable for blending with transportation fuels such as diesel<sup>12,16</sup>. The diesel industry has recently consumed 22% of energy supplied to the US transportation sector and accounted for 24% of greenhouse gas (GHG) emissions by the US transportation sector<sup>17,18</sup>. In response to growing environmental concerns, the transportation industry is exploring economical and environmental solutions to reduce its GHG emissions for sustainable growth. A critical step for biocrude commercialization is the production of blendstocks with fuel properties complying with the standards so that conventional distribution infrastructures can be employed<sup>19</sup>.

However, fuel specification analyses and engine tests of blendstocks refined from HTL biocrude oil are limited because of oxygen and nitrogen contents<sup>12,13,20</sup>, fuel stability<sup>19,21</sup>, the distillation properties of HTL biocrude oil<sup>22</sup> and the cost of upgrading HTL biocrude oil<sup>23,24</sup>. Upgrading the HTL biocrude oil to improve its fuel specification therefore is needed. Catalytic upgrading or hydrotreating of the HTL biocrude oil has been extensively studied in the past few years<sup>10,19,25–27</sup>. Without an external hydrogen source, the poor quality of the upgraded HTL biocrude oil remains a major bottleneck for fuel applications<sup>20,24,26,28</sup>. Because of these barriers, there is no literature evaluating the fuel specification and engine performance of (upgraded) HTL biocrude oil converted from wet biowaste.

Here we present an integrated approach that combines distillation with esterification and enables the use of HTL biocrude oil as diesel blendstocks. In contrast to previous upgrading processes (for example, hydrotreating)<sup>10,25,26</sup>, the distillation separated HTL biocrude oil into different fractions with lower viscosities so that

<sup>1</sup>Department of Agricultural and Biological Engineering, University of Illinois at Urbana-Champaign, Urbana, IL, USA. <sup>2</sup>Laboratory of Environment-Enhancing Energy, and Key Laboratory of Agricultural Engineering in Structure and Environment, Ministry of Agriculture, College of Water Resources and Civil Engineering, China Agricultural University, Beijing, China. <sup>3</sup>Department of Mechanical Science and Engineering, University of Illinois at Urbana-Champaign, Urbana, IL, USA. <sup>4</sup>Prairie Research Institute - Illinois Sustainable Technology Center, University of Illinois at Urbana-Champaign, Champaign, IL, USA. \*e-mail: [yzhang1@illinois.edu](mailto:yzhang1@illinois.edu)

further upgrading (esterification) could be more effective. The distillate fractions with the closest physicochemical properties to petroleum diesel were subjected to esterification, which requires neither hydrogen gas nor expensive catalysts. To verify the approach, this study investigated the combustion and emissions of a diesel engine when using both a blended biofuel (containing 10–20 vol% HTL biofuel) and a petroleum diesel. Over the 20 engine conditions, we found 96–100% power output on average and a similar level of pollutant emissions (101–102% NO<sub>x</sub>, 89–91% CO, 92–125% unburned hydrocarbon and 109–115% soot emissions) to petroleum diesel when using blended biofuel.

In this study, we simultaneously created a value-added product from wet biowaste and eliminated a bottleneck in upgrading HTL biocrude to transportation fuel. We proved the feasibility of HTL biocrude converted from wet biowaste to transportation fuel without hydrotreating, and with comprehensive fuel specification analyses and engine tests. Results from this study provide an alternative approach to biowaste-to-energy valorization and bridge the research gap for co-optimizing biofuels and engine technologies.

### HTL feedstock characterization and HTL of wet biowaste

Characterization of HTL feedstocks is shown in Table 1. Swine manure is one of the most well-studied HTL feedstocks. Food processing waste from a salad dressing plant (SDP) was selected as another type of wet biowaste. Swine manure contains average amounts of crude protein, crude fat and lignocelluloses, while SDP is mainly composed of crude fat and non-fibre carbohydrates (Table 1). The composition of swine manure is similar to other types of wet biowaste such as human waste<sup>28</sup>. Thus, swine manure can be considered as a representative of faecal matter, which generally has an optimal thermal condition of 280–350 °C with a 0.5–2 h reaction time under HTL<sup>12,14,28</sup>. Based on previous studies with the same type of biowaste<sup>29</sup>, we converted swine manure at 280 °C with a 2 h reaction time for up-scaled biocrude oil production, which was used for further distillation and characterizations.

In contrast, the composition of SDP resembles greasy biowaste such as slaughterhouse waste<sup>28</sup> and rendered animal fat<sup>30</sup>. SDP was considered a representative of biowaste from the food processing industry, which typically has an optimal thermal condition of 250–300 °C with a 0.5 h reaction time under HTL<sup>28</sup>. We also conducted a series of HTL tests to determine the optimum reaction conditions (260 °C for 0.5 h) for up-scaled biocrude oil production from SDP. More details are available in Supplementary Table 1. Mineral compositions of swine manure and SDP were also characterized (Supplementary Table 2).

### Distillation of biocrude converted from wet biowaste

Biocrude oils converted from food processing waste (SDP, Fig. 1a) and swine manure (Fig. 1d) were distilled into several distillates. Distillation separated 75% and 41% of distillates from SDP- and swine manure-derived HTL biocrude, respectively, when heated from room temperature to 400 °C. The distillates from SDP-derived biocrude oil (SDP distillates) contained 73 wt% oil and 2 wt% moisture contents, while the distillates from swine manure-derived biocrude oil (swine manure distillates) contained 28 wt% oil and 16 wt% moisture contents (Supplementary Table 3). Additionally, the SDP- and swine manure-derived biocrude oil contained 11 and 42 wt% distillation residues, respectively. The characterizations of the distillation residues are also available in Supplementary Table 3. About 11 and 15 wt% of the SDP- and swine manure-derived biocrude oil, respectively, were lost during distillation. Optimization of the distillation is needed for an up-scaled process in future studies.

### Analyses of distillate fractions

We have characterized distillate fractions separated from SDP- and swine manure-derived HTL biocrude (Fig. 1 and Supplementary

**Table 1 | Chemical and elemental compositions of swine manure and food processing waste used in this study (dry weight basis, dw%)**

Compositions (dw%) <sup>a</sup>	Swine manure <sup>b</sup>	Food processing waste from a SDP
Crude protein	24.3 ± 1.6 (n = 5)	2.76
Crude fat	19.9 ± 1.6 (n = 5)	40.8
Hemicellulose	26.6 ± 2.4 (n = 5)	ND <sup>d</sup>
Cellulose	5.1 ± 3.2 (n = 5)	ND <sup>d</sup>
Lignin	2.9 ± 1.9 (n = 5)	ND <sup>d</sup>
Non-fibre carbohydrates <sup>c</sup>	6.4 ± 4.5 (n = 5)	50.27
Ash content	14.3 ± 2.0 (n = 5)	6.17
C	41.1 ± 0.3 (n = 2)	54.0 ± 1.6 (n = 2)
H	5.42 ± 0.1 (n = 2)	7.93 ± 0.3 (n = 2)
N	3.36 ± 0.1 (n = 2)	0.57 ± 0.01 (n = 2)
O <sup>b</sup>	50.1	37.5

<sup>a</sup>Reported by dry weight basis. <sup>b</sup>Average values were reported based on the previous studies using the same type of swine manure<sup>10,47,53</sup>. <sup>c</sup>Calculated by difference (that is, non-fibrous carbohydrate (%) = 100 - crude fat (%) - crude protein (%) - hemicellulose (%) - cellulose (%) - lignin (%) - ash content (%); O (%) = 100 - C (%) - H (%) - N (%)). <sup>d</sup>Not detected.

Table 3). Density, viscosity and elemental compositions of jet fuel and diesel were also measured for comparison. Viscosity plays an important role in the fuel injection, atomization and combustion processes<sup>31</sup>. Figure 1b,e demonstrates that the viscosities of the HTL distillates generally increased as the distillation temperature increased. The SDP distillates recovered at 218–310 °C and the swine manure distillates recovered at 183–196 °C presented the closest viscosities to those of diesel (Fig. 1b,e). The viscosities of SDP distillates generally increased with the distillation temperature. In contrast, for swine manure distillates, their viscosities first increased in fractions recovered at 99–161 °C (Supplementary Table 3) and then decreased in the fractions recovered at 161 °C–183 °C, which could be attributed to the reduction of phenolic compounds (Supplementary Table 5). For example, the viscosity of phenol at room temperature (12 mm<sup>2</sup> s<sup>-1</sup>)<sup>32</sup> was almost four times that of diesel (3.75 mm<sup>2</sup> s<sup>-1</sup>). Subsequently, the viscosities of swine manure distillates increased again in the fractions recovered at 183–189 °C. This could be due to the higher concentration of fatty acids and fatty esters<sup>32</sup> (for example, hexadecanoic acid) in the fraction recovered at 183–189 °C than that in the fraction recovered at 161–183 °C. The viscosity decreased again in the fractions recovered at 189–196 °C, possibly from the reduction of phenolic compounds.

We also calculated higher heating values (HHV) and measured the carbon (C), hydrogen (H), nitrogen (N) and oxygen (O) contents of SDP and swine manure distillates (Fig. 1). The SDP distillates recovered at 233–310 °C and the swine manure distillates recovered at 161–196 °C presented similar HHV and carbon and hydrogen contents to those of transportation fuels. Notably, the SDP distillates recovered at 233–310 °C demonstrated the closest HHV and levels of carbon, hydrogen and nitrogen to those of transportation fuels. The reduction of the oxygen contents of swine manure distillates results primarily from the removal of water (Fig. 1e).

Relative concentrations of each chemical in the two HTL distillates are shown in Supplementary Tables 4 and 5. Gas chromatography–mass spectrometry (GC–MS) results show that the major compounds in the SDP distillates were hydrocarbons and fatty acid derivatives (Fig. 1c and Supplementary Table 4). The SDP distillates recovered at 233–310 °C mainly contained alkanes and alkenes with carbon numbers of 8–19, which were in the range for jet fuel (10–14)<sup>33</sup> and diesel (8–21)<sup>34</sup>. These fractions also contained saturated and unsaturated fatty acids with carbon numbers of 6–18.

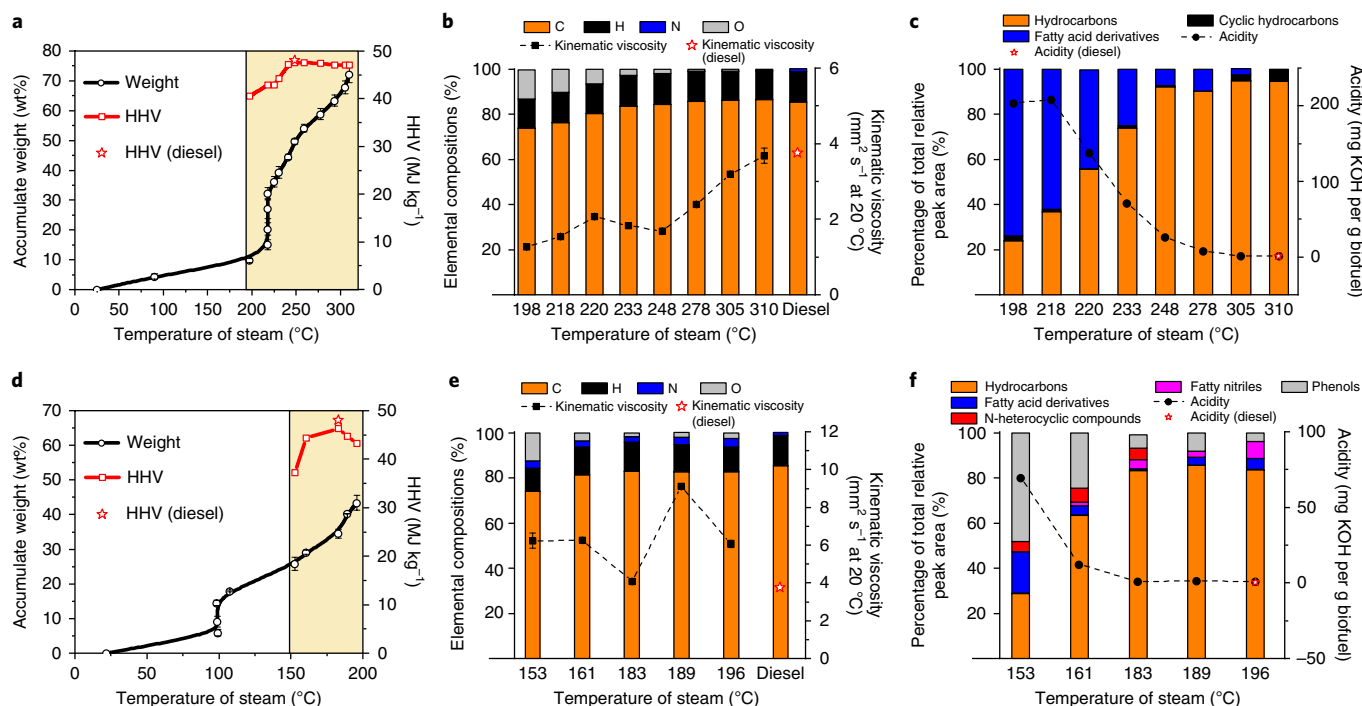


**Fig. 1 | Distillation of SDP- and swine manure-derived biocrude oil. a**, Distillation characteristics ( $n \geq 3$ ) and HHV of SDP-derived biocrude oil. **b**, Elemental compositions ( $n \geq 2$ ) and viscosity ( $n \geq 3$ ) of SDP distillates. **c**, Chemical compositions ( $n = 1$ ) and acidity ( $n \geq 3$ ) of SDP distillates. **d**, Distillation characteristics ( $n \geq 3$ ) and HHV of swine manure-derived biocrude oil. **e**, Elemental compositions ( $n \geq 2$ ) and viscosity ( $n \geq 3$ ) of SW distillates. **f**, Chemical compositions ( $n = 1$ ) and acidity ( $n \geq 3$ ) of SW distillates.

Upgrading would be needed to modify these fatty acids. The swine manure distillates recovered at 161–196 °C mainly contained hydrocarbons and phenols (Fig. 1f and Supplementary Table 5). Alkanes with carbon numbers of 10–18 in these swine manure distillates were suitable for transportation fuel application<sup>33,34</sup>, while phenols, fatty acids, nitrogen-heterocyclic compounds and fatty nitriles needed upgrading. In particular, phenols and fatty acids would lead to an undesirable high acidity in fuel application.

The SDP and swine manure distillates contained fatty acids and phenols that may cause a relatively high acidity for fuel application (Fig. 1c,f). For the SDP distillates, the acidity (reduced from 208 mg KOH per g to 1 mg KOH per g) decreased as the distillation temperature increased. However, the acidity of SDP distillates was much higher than the maximum value (0.3 mg KOH per g) for biodiesel application<sup>35</sup>. The high acidity levels in the light SDP distillates (recovered at 198–233 °C) were mainly due to the presence of organic acids such as acetic acid, hexanoic acid and octadecenoic acid. More details are available in Supplementary Table 4. Therefore, upgrading SDP distillates to reduce their acidity was necessary. In contrast, the acidity of the swine manure distillates was primarily due to phenols and organic acids, making swine manure distillates more complex to upgrade than the SDP distillates.

Considering the distillation characteristics, viscosities, densities, heating values and the elemental and chemical compositions of various types of distillates, the SDP-derived distillates were selected to demonstrate their suitability for diesel blendstocks.

### Upgrading the distillates from SDP-derived biocrude oil

Esterification is an effective method to reduce the acidity of high free fatty acid (FFA) containing bio-oil from 40 mg KOH per g to <1 mg KOH per g<sup>36,37</sup>. The distillate fractions recovered at 233–278 °C from SDP-derived biocrude were combined for esterification because of their moderate acidities (35.3 mg KOH per g on average)

and similar densities (816 kg m<sup>-3</sup> on average) and energy contents (47 MJ kg<sup>-1</sup> on average) to petroleum diesel. We have conducted an orthogonal array design (OAD) with three levels (Supplementary Tables 11 and 12) to investigate the effects of reaction temperature, reaction time, catalyst loadings and molar ratio of distillates to methanol on the acid-catalysed conversion of FFA to methyl esters. The yield and acidity of esterified oil samples are summarized in Fig. 2a. The OAD tests show that the lowest acidity was achieved at 50 °C for 2 h with 2 wt% H<sub>2</sub>SO<sub>4</sub> and 1/15 molar ratio of SDP distillates to methanol.

The OAD determined the influence of the process variables on the yield and acidity of esterified SDP distillates and allows us to select process variables that maximize esterification yield or minimize acidity. Through OAD, one can compute the average value ( $k$ ) of an interested property (such as acidity) at a fixed value of a specific process variables (such as time). As an example, the acidity for the three experiments at the 0.5 h level was 7.28 (condition 1), 1.60 (condition 4) and 2.76 (condition 7), so that the mean value of acidity at level 1 for time was 3.88 (Fig. 2a and Supplementary Table 6). In this example, although the time was fixed at 0.5 h to generate these acidities, all other variables were varied at three levels. The influences of reaction temperature, catalyst loading and molar ratio of feedstocks to methanol, thus, were reflected in this particular data set. We have calculated the mean values for yield and acidity at three levels of the investigated process variables. Supplementary Table 6 shows the mean values ( $k_1$ ,  $k_2$  and  $k_3$ ) for different properties at levels 1, 2 and 3 of each variable investigated. The larger the range of the process variable (for example, time), the more influence the specific process variable had on the property of interest (for example, acidity). In summary, a longer reaction time and a higher molar ratio of feedstocks to methanol were preferred to achieve a higher esterification yield; a higher temperature favours a forward reaction and thus can reach a lower acidity. However,

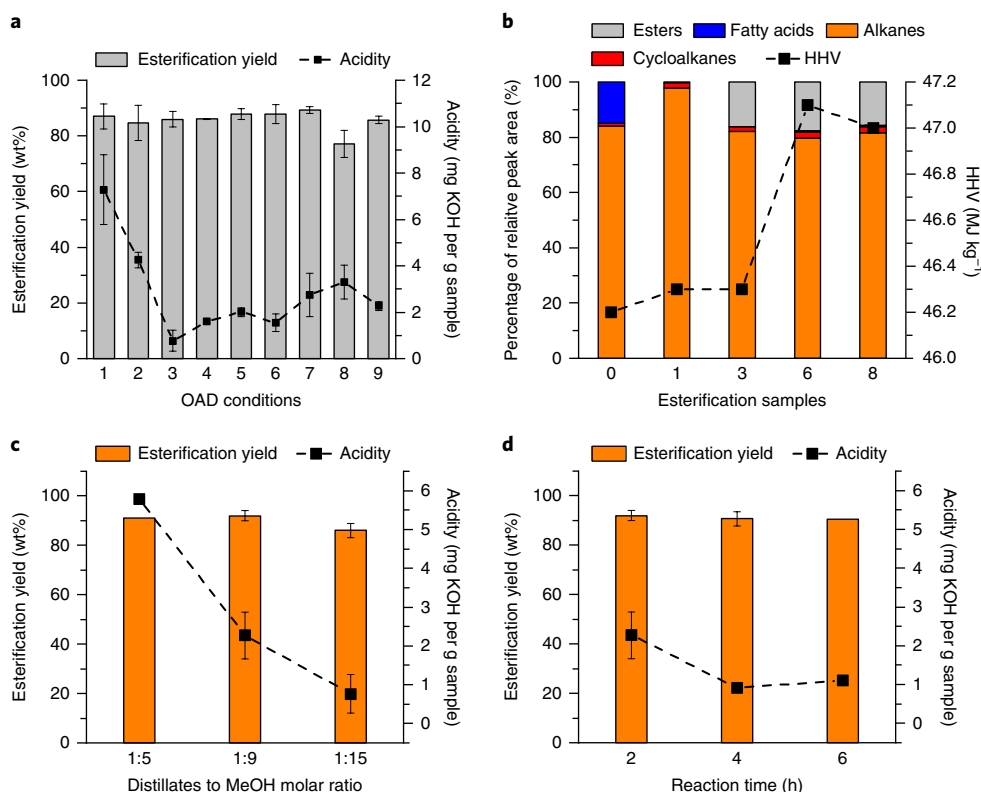


**Fig. 2 | Upgrading of SDP distillates.** **a**, Yield ( $n \geq 2$ ) and acidity ( $n \geq 2$ ) of the esterified samples through OAD tests (detailed OAD conditions can be found in Supplementary Table 12). **b**, Chemical composition of esterified samples with the lowest (obtained at conditions 3 and 6) and highest acidities (obtained at conditions 1 and 8), as well as that before esterification (condition 0) ( $n = 1$ ). **c**, The effect of distillates to methanol molar ratio on the yield and acidity of esterified samples at 50 °C for 2 h with 2 wt%  $\text{H}_2\text{SO}_4$  ( $n \geq 2$ , except for the distillates to MeOH molar ratio of 1:5). **d**, The effect of reaction time on the yield and acidity of esterified samples ( $n \geq 2$ , except for the reaction time of 6 h).

an excessively high temperature (>65 °C) is unfavourable because methanol would be vaporized over its boiling point<sup>36,37</sup>.

Esterified samples that presented the highest (conditions 1 and 8 in Fig. 2a) and the lowest acidities (conditions 3 and 6 in Fig. 2a) were subjected to elemental (Supplementary Table 7) and GC–MS analyses (Fig. 2b) to confirm their energy contents and chemical compositions after esterification. Supplementary Table 8 also includes the chemical compounds in these esterified samples. We validated that the energy contents of esterified samples increased (from 46 to 47 MJ kg<sup>-1</sup>) due to the increasing carbon and hydrogen contents attributed to successful conversions of fatty acid methyl esters (Fig. 2b and Supplementary Table 7). GC–MS analysis verified that esterified samples obtained at conditions 3 and 6 contained higher concentrations of fatty acid methyl esters (Supplementary Table 8) than those at the experimental conditions 1 and 8. This indicates that an effective esterification was realized at conditions 3 and 6.

Through the OAD test, we have identified that reaction time and the molar ratio of distillates to methanol are the major variables affecting the yield and acidity of esterified samples (with larger ranges of  $k$  in the OAD tests). Therefore, we have explored lower molar ratios of SDP distillates to methanol (Fig. 2c) and longer reaction times (Fig. 2d) than the investigated range of the OAD test. A reaction temperature of 50 °C was selected because lower reaction temperatures are preferred. A 2 wt%  $\text{H}_2\text{SO}_4$  was chosen for additional tests to minimize the catalyst ( $\text{H}_2\text{SO}_4$ ) needed during esterification. The molar ratio of SDP distillates to methanol was reduced from 1/15 (optimal conditions from the OAD test) to 1/5 at 50 °C for 2 h with 2 wt%  $\text{H}_2\text{SO}_4$  (Fig. 2c). The acidity of the esterified sample increased from 0.8 to 2.3 and then to 5.8 mg KOH per g sample.

The maximum acidity for a B10 biodiesel (10% biodiesel blend) is 0.3 mg KOH per g sample<sup>35</sup>. If the esterified SDP distillates are to be blended with another 90% of petroleum diesel (~0 mg KOH per g sample) and used as a B10 biodiesel, the maximum acidity of the esterified SDP distillates would be 3.0 mg KOH per g sample. Hence, a 1/9 molar ratio of SDP distillates to methanol was selected for further investigation regarding the effect of reaction time (Fig. 2d). As the reaction time increased from 2 to 4 h and then to 6 h, the acidity of the esterified sample decreased from 2.3 to 0.9 and then increased to 1.1 mg KOH per sample, while the yield was around 90–92 wt%. Thus, a 4 h reaction time was selected to prepare esterified SDP distillates for fuel specification analysis and diesel engine tests.

### Fuel specification analysis and diesel engine tests

Esterified samples (from the distillate fractions recovered at 233–278 °C) plus the distillate fraction recovered at 305 °C were used to formulate a diesel blend with petroleum diesel. Two blends were tested: HTL10 (containing 10 vol% of the HTL distillates) and HTL20 (containing 20 vol% of the HTL distillates). According to the literature<sup>21,31,38</sup>, specifications including viscosity, acidity, sulfur content, cetane number, lubricity and surface tension are relatively important for bio-derived diesel blendstocks. Although the surface tension is not specified in the ASTM International standard (D7467) for B6–B20 biodiesel<sup>35</sup>, it is an important fuel property that affects atomization in diesel engines<sup>39</sup>. As Table 2 shows, the acidity, surface tension, cetane number, lubricity and oxidation stability of HTL10 and HTL20 met the ASTM criteria for biodiesel application.

The cetane number is a critical dimensionless value indicating the readiness of the fuel to auto-ignite when injected into a diesel engine<sup>31</sup>.

**Table 2 | Fuel specification analysis of different drop-in diesel blendstocks and regular diesel**

Fuel specification property	Upgraded SDP		Biodiesel <sup>a</sup>	Camelina oil methyl esters <sup>b</sup>	Butanol <sup>c</sup>	Diesel
	HTL10	HTL20	B6-B20	B10	B100	N/A
Percentage of diesel blendstocks (numbers shown after HTL or B)						
Viscosity (at 20 °C, mm <sup>2</sup> s <sup>-1</sup> ) <sup>d</sup>	3.737 ± 0.01	3.050 ± 0.02	1.9–4.1	2.42 ± 0.01 <sup>e</sup>	2.63	3.746 ± 0.02
Acidity (mg KOH per g) <sup>f</sup>	0.10 ± 0.004	0.29 ± 0.05	<0.3	0.03	NA <sup>g</sup>	NA <sup>g</sup>
Sulfur content (ppm)	17 <sup>h</sup>	NA <sup>g</sup>	<15	0.3	NA <sup>g</sup>	<15 <sup>a</sup>
Existent gum (wt%) <sup>i</sup>	0.17 ± 0.01	0.21 ± 0.02	NA <sup>g</sup>	NA <sup>g</sup>	NA <sup>g</sup>	0.63 ± 0.06
Surface tension (at 24 °C, mN m <sup>-1</sup> )	27.2 ± 0.1	27.0 ± 0.0	NA <sup>g</sup>	27.6 ± 0.1	NA <sup>g</sup>	27.3 ± 0.1 <sup>b</sup>
Cetane number	44.2	43.6	>40	52.8 (B100) <sup>j</sup>	25	41.4 <sup>b</sup>
Wear scar diameter for lubricity (µm)	364	324	<520	142 ± 7	NA <sup>g</sup>	571 ± 5 <sup>b</sup>
Oxidation stability/oil stability index (h)	>48	>48	≥6	17 ± 0.1	NA <sup>g</sup>	>24 <sup>b</sup>

HTL10 and HTL20, respectively, represent 10 vol% and 20 vol% upgraded distillates in petroleum diesel. <sup>a</sup>According to ASTM D7467 (B6-B20 S15). <sup>b</sup>Modified from Moser and Vaughn<sup>38</sup>. <sup>c</sup>Adapted from Liu et al.<sup>34</sup>. <sup>d</sup>Measured using a Cannon–Fenske Viscometer (ASTM D445). <sup>e</sup>Measured at 40 °C. <sup>f</sup>According to ASTM D664. <sup>g</sup>Not applicable. <sup>h</sup>Measured by ICP analysis. <sup>i</sup>Modified from ASTM D381, heating the sample in the furnace from room temperature to 240 °C for 60 min. <sup>j</sup>Measured as 100% biodiesel.

A high cetane number indicates a low ignition delay before combustion and hence is favoured. In this study, the cetane number decreased from 44.2 to 43.6 as the addition of HTL distillates increased from 10 to 20 vol%. HTL distillates may contain chemicals that are hard to ignite. For instance, aromatics and olefins have a low cetane number. According to GC–MS analysis, the esterified SDP distillates contained indene derivatives, which could possibly lead to a low cetane number (Supplementary Table 8). A similar phenomenon regarding combustion behaviour of olefins has been reported previously<sup>40</sup>.

The lubricity of a fuel indicates its ability to reduce wear and friction<sup>31</sup>. Poor lubricity leads to severe wear problems because the fuel injection system is lubricated by the fuel itself. For most petroleum fuels, viscosity is correlated to lubricity<sup>31</sup>. As Table 2 shows, the wear scar diameter for lubricity and viscosity decreased by 11 and 18%, respectively, when the addition of HTL distillates increased from 10 to 20 vol%. A lower wear scar diameter means a higher lubricity. Because HTL distillates from SDP-derived biocrude contained hydrocarbons with smaller carbon chains (for example, decane) than petroleum diesel, the viscosities of the blends (HTL10 and 20) were reduced. For instance, the viscosity of decane is 0.8 mPa s and that of tetradecane is 2.1 mPa s<sup>32</sup>.

The oxidation stability of biodiesel is linked to the presence of unsaturated compounds, particularly unsaturated fatty acid methyl esters and fatty acids, because they tend to degrade over time in storage<sup>38</sup>. HTL10 and HTL20 demonstrated an advantageous oxidation stability of more than 48 h, which is much longer than that of the conventional biodiesel (for example, Camelina oil methyl esters). There was no rapid oxidation in HTL10 and HTL20.

The existent gum content was measured to understand if there were any heavy components in the fuel samples. Because of the low existent gum content of HTL10 and HTL20, we did not measure further biodiesel specifications such as ash content and metals, which are typically contained in the gum fraction.

Sulfur content (S) was measured to understand if HTL10 meets the ASTM criteria for ultralow diesel fuel application (S content < 15 ppm). The sulfur content for HTL10 was 17 ppm (Table 2). This result indicates that the sulfur level of the SDP-derived distillates was higher than the ASTM standard requirement for ultralow diesel application. Desulfurization processes such as adsorption and extraction are suggested to reduce the sulfur level<sup>41</sup>. However, this is beyond the scope of this study. Alternative end products to consider could be bunker fuels (S content < 500 ppm) and fuel oils in various burners (S content < 5,000 ppm), which have less severe sulfur requirements<sup>35</sup>.

We have conducted diesel engine tests with HTL10, HTL20 and diesel to demonstrate the feasibility of HTL distillates as diesel blendstocks (Fig. 3). We have selected three engine speeds (1,200, 1,500 and 2,000 r.p.m.), three fuel injection loads (15, 20 and 25 mg fuel injected per cycle) and four injection timings (12, 8, 4 and 0 crank angle degrees before top dead centre) to evaluate how they may affect the engine performance and emissions (Supplementary Table 9). The diesel engine tests presented in this study serve as evidence that wet biowaste can be converted to high-value energy. Optimizing engine efficiency and emissions are beyond the scope of this study.

In the engine tests, HTL10 and HTL20 achieved competitive power generation (96–100%) with regular diesel (Fig. 3a). This shows that upgraded HTL biocrude oil distil fractions can be a promising diesel blendstock compared to other diesel blendstocks such as butanol, which generally has misfire issues under the same diesel engine test conditions<sup>21</sup>. In diesel engines, fuel was injected into the engine cylinder near the end of the compression stroke. As the piston moved closer to the top dead centre, the temperature of the fuel mixture reached the fuel's ignition point, causing the ignition of some premixed quantity of fuel and air that was atomized and vaporized during the ignition delay<sup>42</sup>. The rest of the fuel not involved in the premixed-dominant combustion was consumed in the rate-controlled combustion phase. In this study, a higher amount of soot indicates that premixed combustion was a minor combustion mechanism. Instead, a rate-controlled combustion was the major mechanism (Fig. 3b).

Figure 3c–e shows that using HTL10 and HTL20 led to a similar level of pollutant emissions (101–102% NO<sub>x</sub>, 89–91% CO, 92–125% unburned hydrocarbon and 109–115% soot emissions) as regular diesel. Specifically, we found that the emission of CO from HTL distillates was much lower than that from regular diesel over the tested diesel injection timing when the engine speed was at 1,200 r.p.m. with the fuel injection loading of 25 mg fuel per stroke (conditions 9–12, Fig. 3d). This is due to the higher oxygen contents (0.2 wt%) of HTL distillates that allow diesel to combust more completely.

### Energy and GHG emissions calculations

HTL processing of wet biowaste is an emerging technology that shows promising potential. However, the HTL biocrude must be upgraded for transportation fuels. Major bottlenecks exist, including energy efficiency and the GHG footprint of the upgrading process. The approach of HTL integrated with distillation plus esterification proved several advantages over the existing

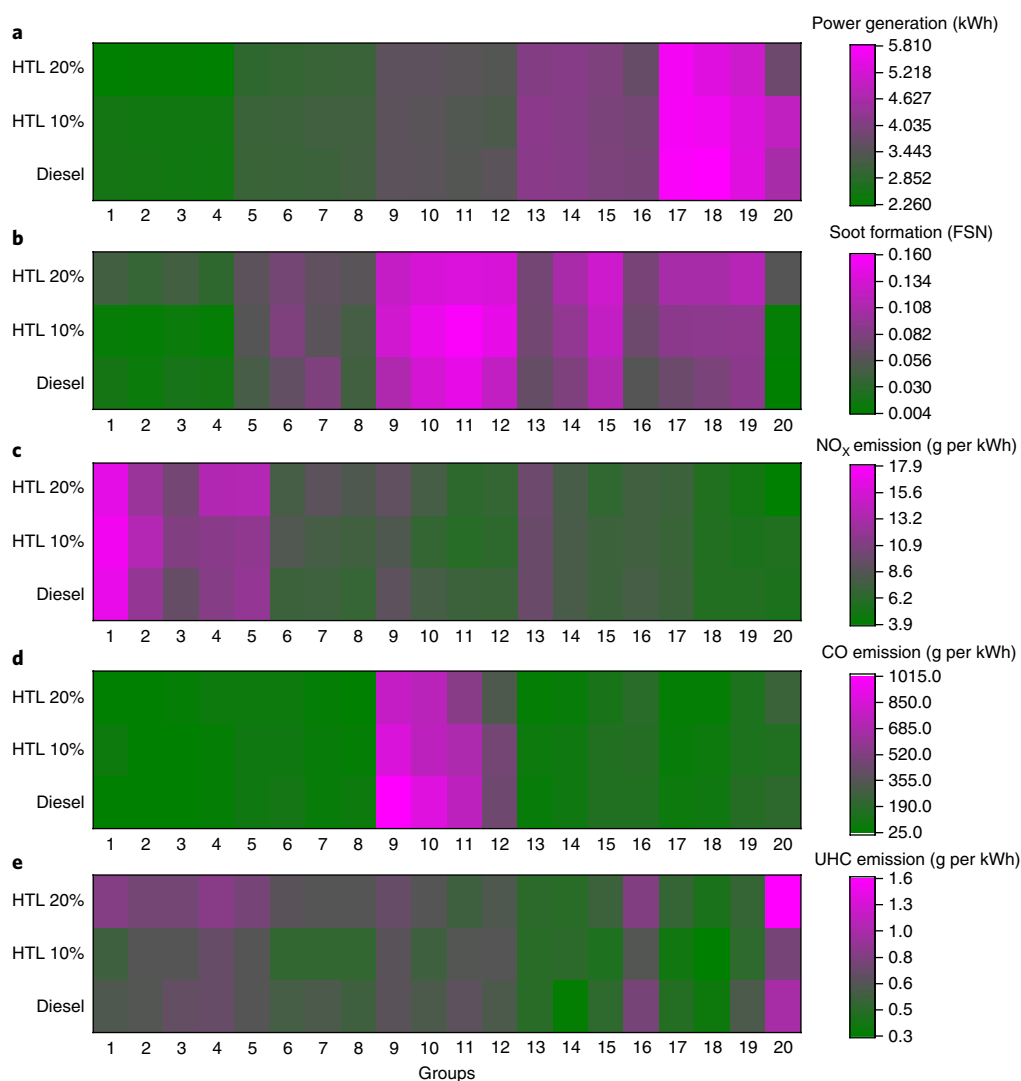


**Fig. 3 | Power generations and pollutant emissions under all diesel engine test conditions.** **a–e**, The effects of engine speed, injection timing and injection loading on power generation (**a**), soot formation (**b**),  $\text{NO}_x$  emission (**c**), CO emission (**d**) and unburned hydrocarbon (UHC) emission (**e**) from drop-in diesel blend prepared with HTL distillates. The diesel engine was operated at 1,200, 1,500 and 2,000 r.p.m. under different fuel injection timings with 15, 20 and 25 mg of fuel per stroke. Fuel injection timing is governed by the crank angle (CA, in degrees) before top dead center (BTDC) in a diesel engine. Thus, CA BTDC of  $0^\circ$ ,  $4^\circ$ ,  $8^\circ$  and  $12^\circ$  have been explored in this study. In general, a diesel engine performs at  $0^\circ$  CA BTDC to reach the highest power output, but running at  $0^\circ$  CA BTDC would result in an incomplete pre-mixing as a trade-off<sup>21</sup>.

waste-to-energy technologies. Our data (Table 3 and Supplementary Table 10) indicate that this approach has a 3–5 times lower process energy input than HTL with hydrotreating and conventional lipid extraction (from dry feedstock)<sup>3,24</sup> and a higher energy recovery ratio (energy output divided by energy input, which includes the energy of biowaste feedstock and processing) than HTL plus hydrotreating, lipid extraction, incineration or landfilling<sup>3,24,43–45</sup>. This is primarily because the approach does not require dry feedstocks and an external hydrogen source. As a result of a lower process energy input, the overall GHG emission is lower. Although HTL integrated with distillation plus esterification has a higher energy input than anaerobic digestion and producing diesel from petroleum, its energy recovery ratio is much higher and its GHG emission is similar<sup>20,24,45,46</sup>.

## Conclusion

In summary, HTL integrated with the combined distillation and esterification allows for an efficient use of wet biowaste. Fuel specification analysis and engine tests with diesel blends (HTL10 and

HTL20) indicate promising results in terms of energy efficiency and air emissions. With qualified cetane numbers ( $>40$ ), lubricities ( $<520\ \mu\text{m}$ ) and oxidation stabilities ( $\geq 6\ \text{h}$ ), HTL10 and HTL20 result in competitive power generation (96–100%) and similar levels of pollutant emissions (101–102%  $\text{NO}_x$ , 89–91% CO, 92–125% unburned hydrocarbon and 109–115% soot emissions), compared to petroleum diesel. HTL integrated with distillation and esterification (0.8) has a higher energy recovery ratio than HTL plus hydrotreating (0.4), anaerobic digestion (0.1–0.6) and producing diesel from petroleum (0.3). Through a combined distillation and esterification approach, the energy consumption embedded within food waste can be utilized, allowing for the creation of a value-added product from food waste and the elimination of a bottleneck in HTL biocrude commercialization.

## Methods

**Feedstock.** Swine manure was sampled from the floor of a grower-finisher barn. Food processing waste was sampled from a full-scale SDP. Before HTL

**Table 3 | Estimated energy demand, energy recovery ratio (energy output/energy input) and GHG emissions of the production of diesel and different biowaste-to-energy methods**

	Process energy input (MJ kg <sup>-1</sup> feedstock)	Energy recovery ratio <sup>a</sup>	GHG (kg CO <sub>2</sub> kg <sup>-1</sup> product) during the process	Product
Diesel	2.5	0.3	0.2	Fuel
Landfill	0.03–0.04	0	0.9–1.8	Methane
Incineration	0.02–0.03	2.3 × 10 <sup>-4</sup>	2.0	Electricity
Anaerobic digestion	0.7	0.1–0.6	0.1	Methane
Lipid extraction	3.7 (wet)–17 (dry)	0.4 (dry)–0.8 (wet)	1.1 (wet)–7.4 (dry)	Biodiesel
HTL + hydrotreating	8.9	0.4	0.4	Diesel blendstock
HTL + distillation + esterification (present study)	3.2	0.8	0.2	Diesel blendstock

Only the energy demand and GHG emissions during the production process were compared (those for implementing the entire scheme are excluded). <sup>a</sup>Defined as the energy output divided by the energy input. The energy output is defined as the (bio)fuel (or biogas) yield multiplied by the energy content of the (bio)fuels (or biogas). The energy input includes the energy of biowaste feedstocks and the energy input for processes. For example, the energy output of the present study is the upgraded biocrude oil yield multiplied by the energy content of the upgraded biocrude oil. The energy input includes the energy content of SDW biowaste and the energy needed for HTL, distillation and esterification.

experiments, the feedstocks were stored in a refrigerator at 4 °C and pulverized using a commercial blender (Waring Commercial). We measured the total solid content as the dry residue at 105 °C after 24 h drying. We evaluated the contents of crude protein (AOAC 990.03), crude fat (AOAC 954.02) and lignin (AOAC 973.18) using AOAC standard methods. We determined the acid and neutral detergent fibres by using Ankom Technology standard methods (MWL DF 021)<sup>10,12,47</sup>. Elemental analysis of feedstock was operated by a CHN analyser (Exeter Analytical) and duplicate analysis was conducted for each sample and the average value was reported. ICP analysis was employed to measure the contents of total sulfur (S), phosphorus (P), potassium (K), magnesium (Mg), calcium (Ca), sodium (Na), iron (Fe), manganese (Mn), copper (Cu) and zinc (Zn) in the feedstocks, according to the Association of Official Analytical Chemists (AOAC) standard methods (AOAC 985.01).

**HTL experiments and product separation.** The HTL experiments were conducted using a continuous reactor (Snapshot Energy)<sup>48</sup>. Briefly, we carried out the HTL reaction at the optimum conditions to convert the biowaste into biocrude oil (for swine manure, 280 °C and 2 h reaction time; for SDP, 260 °C and 0.5 h reaction time)<sup>11,20,48</sup>. The reactor was sealed and purged with nitrogen gas at least three times to remove the residual air in the reactor. Nitrogen gas was again added to the reactor to build a 0.69 MPa initial pressure inside the reactor to prevent water from boiling during the tests. After the HTL reaction at the designated temperature and reaction time, the reactor was cooled down to approximately 60 °C using the heat exchangers. The HTL products converted from biowaste, containing both solid and liquid phases, could be separated by decanting because the biocrude oil (solid phase) naturally self-separated from the aqueous products<sup>27,48</sup>. The moisture content of the biocrude oil was measured with a distillation apparatus based on ASTM Standard D95-99<sup>12,13,15</sup>.

**Distillation of biocrude oil.** The distillation was conducted according to the previously reported methods<sup>49,50</sup> and the distillation curves were measured. For each distillation test, approximately 200 g biocrude oil was loaded into a 300 ml round-bottom flask, which was heated with a stirring heating mantle (Azzota SHM-250, LabShops). To avoid quick distillations that could cause ineffective separation and safety issues, the heating rate was set at about 1 °C min<sup>-1</sup>. The biocrude in the flask was homogenized with a stir bar to enhance the heat transfer. To reduce the heat loss, glass wool was wrapped around the distillation equipment. The distillation was conducted under an atmospheric pressure. The vapour distillate was refluxed into an inclined condenser and then condensed by circulating tap water. Distillate fractions at a weight of 10 g (~5 wt% of feed biocrude) each were collected at different distillation temperatures in sequence<sup>49,50</sup>. Distillation experiments were conducted for at least three independent tests with two types of biocrude and average values were reported.

**Upgrading of distillates.** The objective of this part of the study was to develop processes for upgrading distillates from wet biowastes into fuel-grade diesel. Esterification was conducted to reduce the high FFA feedstocks. Distillates with high FFA were converted to esters with methanol and acidic catalysts (Supplementary Fig. 1). A Brønsted acid such as H<sub>2</sub>SO<sub>4</sub> was used for methyl esterification of FFA.

To investigate the effects of reaction temperature, reaction time, catalyst loadings and molar ratio of distillates to methanol on the acid-catalysed conversion of FFA to methyl esters, an OAD with three levels was performed (Supplementary Tables 11 and 12). Previous studies reported that reaction temperatures between 50 and 80 °C, reaction times between 0.5 and 3 h, catalyst loadings of 0.5–5 wt% and molar ratio of feedstocks to methanol between 1/6 and 1/12 are suitable

for converting FFA to methyl esters, depending on the feedstock types<sup>36,37</sup>. As a consequence, reaction temperatures of 50, 60 and 70 °C were used in the present work. Excessively high reaction temperatures were avoided so the methanol would not be boiled and the reaction vessel would not need to be pressurized. Reaction times of 0.5, 1 and 2 h, catalyst loadings of 0.5, 1 and 2 wt% and molar ratios of feedstocks to methanol of 1/5, 1/9 and 1/15 were selected to make the OAD optimization more efficient and economic. Longer reaction times, higher catalyst loading and more methanol were used when necessary. After the reaction, the esterified oil contained water, excess methanol and acid catalysts that needed to be removed. The oil layer was separated from the mixture with a funnel separator and passed over anhydrous Na<sub>2</sub>SO<sub>4</sub>. The yield of esterification was calculated based on the weight of treated oil ( $W_{\text{ester}}$ ) divided by the weight of distillates ( $W_{\text{distillates}}$ ) (that is,  $W_{\text{ester}}/W_{\text{distillates}}$ ). The acidity of esterified oil was measured according to ASTM D7467 standard<sup>36,37,51</sup>. Elemental and GC–MS analyses were conducted on select esterified samples to ensure their fuel quality.

**Analysis of products.** Elemental compositions of biocrude oil and distillates were determined using a CE 440 elemental analyser (Exeter Analytical). The HHV of biocrude oil and distillates were calculated by using the Dulong formula based on the elemental composition:  $\text{HHV} = 0.3383 \times \text{C} + 1.422 \times (\text{H} - \text{O}/8)$ <sup>12,13</sup>. The chemical compositions of distillates (extracted with hexane) were analysed using GC–MS (Agilent Technologies). The internal standard, pentadecanoic acid methyl ester (0.5 μM), was used. The detailed analytical methods have also been described in previous literature<sup>15,25</sup>. Briefly, samples were analysed using a GC–MS system consisting of an Agilent 7890 gas chromatograph, an Agilent 5975 mass selective detector and a HP 7683B autosampler. Gas chromatography was performed on a ZB-5MS capillary column. The inlet and mass spectrometry interface temperatures were 250 °C and the ion source temperature was adjusted to 230 °C. The helium carrier gas was kept at a constant flow rate of 2 ml min<sup>-1</sup>. The temperature programme was 5-min isothermal heating at 70 °C followed by an oven temperature increase of 5 °C per min to 310 °C and a final 10 min hold at 310 °C. The mass spectrometer was operated in positive electron impact mode at 69.9 eV ionization energy at an  $m/z$  50–800 scan range. The spectra of all chromatogram peaks were compared with electron impact mass spectrum libraries (NIST08 and W8N08). Because the response factors for different chemicals can greatly differ, all data were normalized to the internal standard to allow comparison between samples. Regarding a large number of chemicals in each HTL distillate, we have identified chemicals with the signals higher than that of the added internal standard to ensure consistency and efficiency. The instrument variability was within the standard acceptance limit (5%).

**Drop-in fuel preparation and fuel specification analysis.** Distillates derived from SDP were added into diesel to obtain a 10–20 vol% drop-in biodiesel. The fuel specifications including viscosity, density, acidity, surface tension, existent gum content, cetane number, lubricity and oxidation stability of drop-in biodiesel were measured and compared to those of transportation fuel standards. The characterizations of fuel specification were conducted by ASTM D7467 standard and previously reported methods<sup>15,38</sup>.

**Diesel engine tests.** The diesel engine tests were conducted according to the previously reported methods<sup>21</sup>, using an AVL 5402 single-cylinder diesel engine. Key engine specifications are presented in Supplementary Table 13. The engine was coupled to a GE type TLC-15 class 4-35-1700 dynamometer capable of delivering up to 14.9 kW (20 HP) and absorbing up to 26.1 kW (35 HP) at a maximum rotational speed of 4,500 r.p.m. A Dyne Systems DYN-LOC IV controller controlled the dynamometer. A Kistler type 6125B pressure transducer

measured in-cylinder pressure with an AVL 3057-AO1 charge amplifier and was indexed against a crankshaft position signal from a BEI XH25D shaft encoder<sup>21</sup>. Supplementary Fig. 2 illustrates the engine setup schematic. The control and diagnostic parameters in the engine control module were developed and calibrated through a software package (INCA, published by ETAS). We also acquired the data and real-time recording of engine conditions using INCA. An ETAS ES580 interface card was used as the connection between the electronic diesel control and the programme.

**Diesel engine emission analysis.** We measured the nitrogen oxides (NO<sub>x</sub>) by using a non-sampling type meter (Horiba MEXA-720, with the measurement range of 0–3,000 ppm). We sampled the emissions of carbon monoxide (measurement ranges of 0.00–10.00% by volume), carbon dioxide (measurement ranges of 0.00–20.00% by volume) and unburned hydrocarbon (measurement ranges of 0–10,000 ppm) by using a sampling type meter (Horiba MEXA-554JU). More details can be found in the literature<sup>21,52</sup>. Exhaust gas temperature located in the exhaust manifold was measured by a type-K thermocouple.

Soot content was determined by a standard filter paper method<sup>21</sup>. Raw exhaust gases were drawn through a 7/8" round filter paper using a vacuum pump. Rectangular strips of filter papers (Grainger Industrial Supply) were in a filter holder from a Bacharach True-Spot smoke meter. The sampling flow rate was constantly monitored by a flow meter. After the samples were collected, we used a digital scanner to estimate the filter paper blackening.

Paper blackening, PB, is defined as

$$PB = \frac{100 - R_R}{10} \quad (1)$$

where

$$R_R = \left( \frac{R_p}{R_t} \right) \times 100\% \quad (2)$$

$R_p$  is the reflectometer value of sample,  $R_t$  is the reflectometer value of unblackened paper and  $R_p$  is the relative brightness of the sample (relative radiance factor)

We considered the paper blackening value as the filter smoke number at 1 bar and 298 K.

## Data availability

The data that support the findings of this study are available from the corresponding author upon request.

Received: 7 September 2017; Accepted: 9 October 2018;

Published online: 13 November 2018

## References

1. Database of Food and Agriculture Organization of the United Nations (FAO, 2016); <http://faostat3.fao.org/home/E>
2. *Biofuels and Bioproducts from Wet and Gaseous Waste Streams: Challenges and Opportunities* (USDOE, EERE Publication and Product Library, 2017).
3. Lardon, L., Hélias, A., Sialve, B., Steyer, J.-P. & Bernard, O. Life-cycle assessment of biodiesel production from microalgae. *Environ. Sci. Technol.* **43**, 6475–6481 (2009).
4. Xu, L., Brilman, D. W. F., Withag, J. A. M., Brem, G. & Kersten, S. Assessment of a dry and a wet route for the production of biofuels from microalgae: energy balance analysis. *Bioresour. Technol.* **102**, 5113–5122 (2011).
5. Déniel, M., Haarlemmer, G., Roubaud, A., Weiss-Hortala, E. & Fages, J. Energy valorisation of food processing residues and model compounds by hydrothermal liquefaction. *Renew. Sustain. Energ. Rev.* **54**, 1632–1652 (2016).
6. Bank, T. W. 'What a Waste' report shows alarming rise in amount, costs of garbage. *The World Bank* <http://www.worldbank.org/en/news/feature/2012/06/06/report-shows-alarming-rise-in-amount-costs-of-garbage> (2012).
7. Van Minh, H. & Nguyen-Viet, H. Economic aspects of sanitation in developing countries. *Environ. Health Insights* **5**, 63–70 (2011).
8. *OECD Studies on Water Meeting the Water Reform Challenge* (OECD Publishing, 2012).
9. Peterson, A. A. et al. Thermochemical biofuel production in hydrothermal media: a review of sub- and supercritical water technologies. *Energy Environ. Sci.* **1**, 32–65 (2008).
10. Yu, G. *Hydrothermal Liquefaction of Low-Lipid Microalgae to Produce Bio-Crude Oil*. PhD thesis, Univ. Illinois at Urbana-Champaign (2012).
11. He, B., Zhang, Y., Funk, T. L., Riskowski, G. L. & Yin, Y. Thermochemical conversion of swine manure: an alternative process for waste treatment and renewable energy production. *Trans. ASAE* **43**, 1827–1833 (2000).
12. Chen, W.-T. et al. Co-liquefaction of swine manure and mixed-culture algal biomass from a wastewater treatment system to produce bio-crude oil. *Appl. Energy* **128**, 209–216 (2014).
13. Chen, W.-T. et al. Hydrothermal liquefaction of mixed-culture algal biomass from wastewater treatment system into bio-crude oil. *Bioresour. Technol.* **152**, 130–139 (2014).
14. He, B., Zhang, Y., Yin, Y., Funk, T. L. & Riskowski, G. L. Operating temperature and retention time effects on the thermochemical conversion process of swine manure. *Trans. ASAE* **43**, 1821–1825 (2000).
15. Yu, G., Zhang, Y. H., Schideman, L., Funk, T. & Wang, Z. C. Distributions of carbon and nitrogen in the products from hydrothermal liquefaction of low-lipid microalgae. *Energy Environ. Sci.* **4**, 4587–4595 (2011).
16. Gai, C., Zhang, Y., Chen, W.-T., Zhang, P. & Dong, Y. Energy and nutrient recovery efficiencies in biocrude oil produced via hydrothermal liquefaction of *Chlorella pyrenoidosa*. *RSC Adv.* **4**, 16958–16967 (2014).
17. *Inventory of US Greenhouse Gas Emissions And Sinks, 1990–2015* (US Environmental Protection Agency, Office of Policy, Planning, and Evaluation, 2017).
18. *Diesel Fuel Explained: Use of Diesel* (USEIA, 2018); [http://www.eia.gov/Energyexplained/index.cfm?page=diesel\\_use](http://www.eia.gov/Energyexplained/index.cfm?page=diesel_use)
19. Cole, A. et al. From macroalgae to liquid fuel via waste-water remediation, hydrothermal upgrading, carbon dioxide hydrogenation and hydrotreating. *Energy Environ. Sci.* **9**, 1828–1840 (2016).
20. Chen, W.-T. *Upgrading Hydrothermal Liquefaction Biocrude Oil from Wet Biowaste into Transportation Fuel*. PhD thesis, Univ. Illinois at Urbana-Champaign (2017).
21. Lee, T. H., Lin, Y., Meng, X., Li, Y. & Nithyanandan, K. *Combustion Characteristics of Acetone, Butanol, and Ethanol (Abe) Blended with Diesel in a Compression-ignition Engine* SAE Technical Paper 2016-01-0884 (SAE, 2016); <https://doi.org/10.4271/2016-01-0884>
22. Hoffmann, J., Jensen, C. U. & Rosendahl, L. A. Co-processing potential of HTL bio-crude at petroleum refineries—Part 1: fractional distillation and characterization. *Fuel* **165**, 526–535 (2016).
23. Jones, S. B. et al. *Process Design and Economics for the Conversion of Algal Biomass to Hydrocarbons: Whole Algae Hydrothermal Liquefaction and Upgrading* (US Department of Energy, OSTI, 2014); <https://doi.org/10.2172/1126336>
24. Tzanetis, K. F., Posada, J. A. & Ramirez, A. Analysis of biomass hydrothermal liquefaction and biocrude-oil upgrading for renewable jet fuel production: the impact of reaction conditions on production costs and GHG emissions performance. *Renew. Energ.* **113**, 1388–1398 (2017).
25. Zhang, J., Chen, W.-T., Zhang, P., Luo, Z. & Zhang, Y. Hydrothermal liquefaction of *Chlorella pyrenoidosa* in sub- and supercritical ethanol with heterogeneous catalysts. *Bioresour. Technol.* **133**, 389–397 (2013).
26. Duan, P. & Savage, P. E. Catalytic treatment of crude algal bio-oil in supercritical water: optimization studies. *Energy Environ. Sci.* **4**, 1447–1456 (2011).
27. Elliott, D. C. et al. Process development for hydrothermal liquefaction of algae feedstocks in a continuous-flow reactor. *Algal Res.* **2**, 445–454 (2013).
28. Zhang, Y. & Chen, W. T. in *Direct Thermochemical Liquefaction for Energy Applications* (ed. Rosendahl, L.) Ch. 5 (Elsevier, Duxford, 2018).
29. Ocfemia, K., Zhang, Y. & Funk, T. Hydrothermal processing of swine manure to oil using a continuous reactor system: effects of operating parameters on oil yield and quality. *Trans. ASABE* **49**, 1897–1904 (2006).
30. Ikura, M., Kouchachvili, L. & Caravaggio, G. Production of biodiesel from waste fat and grease. In *Proc. World Scientific and Engineering Academy and Society (WSEAS) International Conference on Renewable Energy Sources* (eds Helms, C. & Celikyay, S.) 25–30 (WSEAS, 2007).
31. Lu, Q., Li, W.-Z. & Zhu, X.-F. Overview of fuel properties of biomass fast pyrolysis oils. *Energy Convers. Manag.* **50**, 1376–1383 (2009).
32. Haynes, W. M. *CRC Handbook of Chemistry and Physics* 97th edn (CRC Press, Boca Raton, 2016).
33. Colket, M. et al. Development of an experimental database and kinetic models for surrogate jet fuels. In *45th AIAA Aerospace Sciences Meeting and Exhibit* 8–11 (Aerospace Research Council, 2007); <https://doi.org/10.2514/6.2008-972>
34. Collins, C. D. In *Phytoremediation* (ed. Willey, N.) 99–108 (Humana Press, New York, 2007).
35. *Annual Book of ASTM Standards D7467* (ASTM, 2015).
36. Canakci, M. & Van Gerpen, J. Biodiesel production from oils and fats with high free fatty acids. *Trans. ASAE* **44**, 1429 (2001).
37. Naik, M., Meher, L., Naik, S. & Das, L. Production of biodiesel from high free fatty acid *Karanja* (*Pongamia pinnata*) oil. *Biomass Bioenergy* **32**, 354–357 (2008).
38. Moser, B. R. & Vaughn, S. F. Evaluation of alkyl esters from *Camelina sativa* oil as biodiesel and as blend components in ultra low-sulfur diesel fuel. *Bioresour. Technol.* **101**, 646–653 (2010).
39. Ejim, C., Fleck, B. & Amirfazli, A. Analytical study for atomization of biodiesels and their blends in a typical injector: surface tension and viscosity effects. *Fuel* **86**, 1534–1544 (2007).
40. Ghosh, P. & Jaffe, S. B. Detailed composition-based model for predicting the cetane number of diesel fuels. *Ind. Eng. Chem. Res.* **45**, 346–351 (2006).

41. Demirbas, A., Alidrisi, H. & Balubaid, M. A. API gravity, sulfur content, and desulfurization of crude oil. *Petrol. Sci. Technol.* **33**, 93–101 (2015).
42. Heywood, J. *Internal Combustion Engine Fundamentals* (McGraw-Hill Education, New York, 1988).
43. Zhou, Y., Schideman, L., Yu, G. & Zhang, Y. A synergistic combination of algal wastewater treatment and hydrothermal biofuel production maximized by nutrient and carbon recycling. *Energy Environ. Sci.* **6**, 3765–3779 (2013).
44. Nabavi-Pelesaraei, A., Bayat, R., Hosseinzadeh-Bandbafha, H., Afrasyabi, H. & Chau, K.-w. Modeling of energy consumption and environmental life cycle assessment for incineration and landfill systems of municipal solid waste management—a case study in Tehran Metropolis of Iran. *J. Clean. Prod.* **148**, 427–440 (2017).
45. Opatokun, S. A., Lopez-Sabiron, A., Ferreira, G. & Strezov, V. Life cycle analysis of energy production from food waste through anaerobic digestion, pyrolysis and integrated energy system. *Sustainability* **9**, 1804 (2017).
46. Furuoholt, E. Life cycle assessment of gasoline and diesel. *Resour. Conserv. Recycl.* **14**, 251–263 (1995).
47. Wang, Z. *Reaction Mechanisms of Hydrothermal Liquefaction of Model Compounds and Biowaste Feedstocks*. PhD thesis, Univ. Illinois at Urbana-Champaign (2011).
48. Ocfemia, K., Zhang, Y. & Funk, T. Hydrothermal processing of swine manure into oil using a continuous reactor system: development and testing. *Trans. ASAE* **49**, 533–541 (2006).
49. *Annual Book of ASTM Standards D86-15* (ASTM, 2015).
50. Cheng, D., Wang, L., Shahbazi, A., Xiu, S. & Zhang, B. Characterization of the physical and chemical properties of the distillate fractions of crude bio-oil produced by the glycerol-assisted liquefaction of swine manure. *Fuel* **130**, 251–256 (2014).
51. Leung, D. Y., Wu, X. & Leung, M. A review on biodiesel production using catalyzed transesterification. *Appl. Energy* **87**, 1083–1095 (2010).
52. Lee, T. H. et al. Experimental investigation of a diesel engine fuelled with acetone-butanol-ethanol/diesel blends. In *ASME 2015 Internal Combustion Engine Division Fall Technical Conference V001T002A015* (ASME, 2015); <https://doi.org/10.1115/icef2015-1148>
53. Dong, R. et al. Product distribution and implication of hydrothermal conversion of swine manure at low temperatures. *Trans. ASABE* **52**, 1239–1248 (2009).
54. Liu, H., Lee, C.-F., Huo, M. & Yao, M. Combustion characteristics and soot distributions of neat butanol and neat soybean biodiesel. *Energy Fuels* **25**, 3192–3203 (2011).

## Acknowledgements

We thank USDA, Illinois Sustainable Technology Center and the Snapshot Energy Gift Fund for providing experimental supplies for the research. We are grateful for financial support from the Graduate College of University of Illinois and the Ministry of Education of Taiwan (to W.-T.C.). We thank E. Eves and K. Subedi in the Microanalysis Laboratory (Urbana, IL) for their help on elemental analyses. We also thank A. Ulanov of the Roy J. Carver Biotechnology Center (Urbana, IL) for help received and discussions on GC–MS analysis. We acknowledge B. Banks from the National Center for Agricultural Utilization Research (Peoria, IL) for collecting surface tension data. We are grateful for assistance provided by B. Kunwar, T. Burton, K. Nithyanandan, P. Zhang and M. Swoboda during this project. We also thank M.-H. Lai for help setting up and troubleshooting the distillation apparatus.

## Author contributions

W.-T.C. designed and conducted experiments for distillation and esterification, analysed results from distillation, esterification, fuel specification and engine tests and wrote the manuscript. Y.Z. designed and supervised the overall project and contributed to data analysis and writing of the manuscript. T.L. and C.-F.L. designed and performed engine tests and contributed to experiments about engine tests and their data analysis. Z.W. conducted experiments for distillation and fuel specification and assisted in preparing samples for engine tests. B.S. contributed to data analysis and writing of the manuscript. A.L. performed experiments for distillation and fuel specification and contributed to writing of the manuscript. B.K.S. assisted with distillation experimental design and contributed to fuel specification analysis and writing of the manuscript.

## Competing interests

The authors declare no competing interests.

## Additional information

**Supplementary information** is available for this paper at <https://doi.org/10.1038/s41893-018-0172-3>.

**Reprints and permissions information** is available at [www.nature.com/reprints](http://www.nature.com/reprints).

**Correspondence and requests for materials** should be addressed to Y.Z.

**Publisher's note:** Springer Nature remains neutral with regard to jurisdictional claims in published maps and institutional affiliations.

© The Author(s), under exclusive licence to Springer Nature Limited 2018